SERS spectrum and DFT calculations of 6-nitrochrysene on silver islands

E.A. Carrasco Flores[a], M.M. Campos Vallette[a], R.E.C. Clavijo[a], P. Leyton[a], G. Díaz F.[b,*], R. Koch[c]

[a]*Molecular Spectroscopy Laboratory, Department of Chemistry, Faculty of Science, University of Chile, Casilla 653, Santiago, Chile*
[b]*Faculty of Sciences, Universidad de Playa Ancha, P.O. Box 34-V, Valparaiso, Chile*
[c]*Institute for Pure and Applied Chemistry, University of Oldenburg, P.O. Box 2503, D-26111 Oldenburg, Germany*

Abstract

The interaction of 6-nitrochrysene with silver clusters has been modelled by using density functional theory calculations DFT. The chemical adsorption through the nitro group and the corresponding molecular orientation of the adsorbate on silver clusters can be compared with the experimental results obtained in surface-enhanced Raman scattering (SERS). A good agreement is found between the model computation of the vibrational spectrum of the adsorbate and the experimental SERS.

Keywords: 6-Nitrochrysene; Ag metal islands; SERS spectrum and DFT calculation

1. Introduction

The present work is part of a general study concerning identification of generic polycyclic aromatic hydrocarbons (PAHs) by using surface-enhanced Raman scattering (SERS) under different experimental conditions, with the aid of theoretical simulations in order to improve the interpretation of results. Thus, our main motivation to perform this kind of research is to look for a model representing an adequate surface in which Raman bands of PAHs can be enhanced. The 6-nitrochrysene (6-Nchr) belongs to a family of polycyclic aromatic hydrocarbons (nitro-PAHs), which are common environmental pollutants believe to be involved in carcinogenesis [1]. The vibrational characterisation of the ground electronic state of these compounds is central to use characteristic internal vibrations as probes in their analytical detection using ultrasensitive chemical techniques such as SERS or to follow up the biological activity of molecular moieties (NO_2) [2]. Vibrational studies of 6-Nchr have been partially performed [3–5]. Furthermore, a complete assignment of the infrared and Raman work using infrared and Raman and resonance Raman has been completed and is reported elsewhere [6]. In the present report we present a summary of characteristic vibrational frequencies for three nitro-PAHs in order to provide the background for a discussion of the computational results for 6-Nchr–Ag complexes as shown in Fig. 1. The main goal of the computational approach was to provide an insight into the 6-Nchr–Ag interactions that could explain the observed SERS spectra on silver nanoparticles. The research was prompted by the fact that under certain experimental conditions 1-nitropyrene and 2-nitrofluorene in concentrations less than 10^{-6} M interact with the surface through the nitro group [7,8]. Theoretical density functional theory (DFT) calculations for the model systems were performed at the SVWN/LANL2DZ level of theory to complete the information about the energetic of the adsorbate–substrate interaction for an approximate molecular model and to gain

* Corresponding author.
E-mail address: gdiazf@upa.cl (G. Díaz F.).

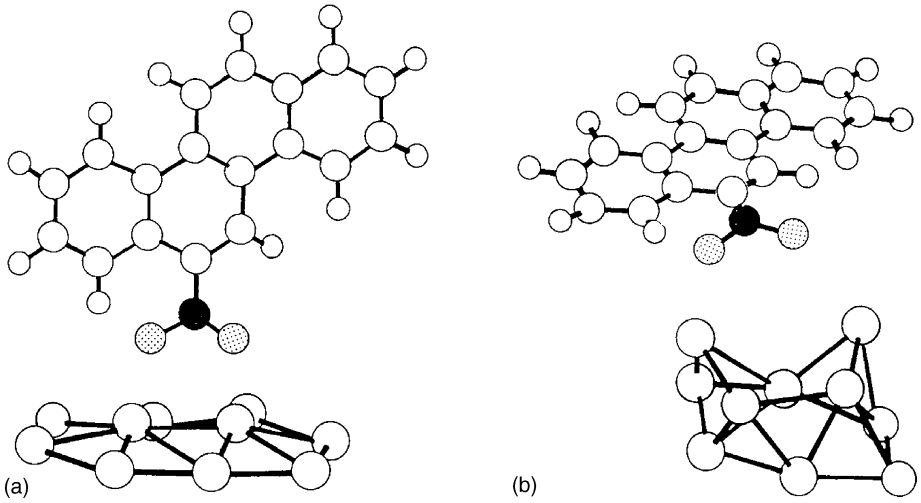

Fig. 1. Molecular structure of 6-nitrochrysene and metal-molecule model for the interaction 6-nitrochrysene–Ag surface: (a) fixed geometry (frozen), (b) optimised geometry (free).

more insight into the spectral assignment of the non-frozen adsorbates.

2. Experimental

6-Nchr was purchased from Aldrich Chemical Company and used without further purification. Metals for surface preparations were purchased from Aldrich (99.99% purity).

The Raman spectra were recorded with a micro-Raman Renishaw system 2000 by using the 514.5, 633 and 780 nm laser lines. The laser power at the sample location was varied from 10 μW to a maximum of 1 mW. Silver island films of 6 and 10 nm mass thickness were deposited in a Balzers vacuum system evaporator using a Balzers BSV 080 glow discharge evaporation unit. The silver island films were deposited onto a preheated glass substrate (200 °C). Thin solid 6-nitrochrysene films were then deposited onto the silver island films. Organic films were 10 and 20 nm mass thicknesses. During thin film deposition, the background pressure was nominally 10^{-6} Torr and the deposition rate was monitored using an XTC Inficon quartz crystal oscillator. A UV HeCd laser line at 325 nm was used to obtain the resonance Raman scattering of the neat material.

3. Theoretical computations

3.1. Molecular models

In the course of our study, we have investigated several models for the metal surface consisting of 2, 4 and 10 Ag atoms. In a recent paper we have discussed the importance of a detailed description of the surface [8]. The optimised geometry of the adsorbate substrate system was calculated in different ways: first, keeping frozen the whole system in order to obtain theoretical frequencies and Raman activities; in this case, the adsorbate was oriented perpendicular to the surface, being the interaction verified through the oxygen atoms of the nitro group. In a second case, the interaction between the molecule and the surface cluster (geometry of the whole system) was also optimised leaving the system to evolve freely until to get a geometry representing the lowest energy. Also, we have optimised the geometry of the interacting system by keeping frozen only the surface. In the second and third cases the molecule trends to be out off perpendicularity in relation to the surface cluster. The electroneutral Ag cluster was initially built with the current bond parameter for this metal representing a 0 0 1 face. In all cases the geometry optimisation of 6-Nchr shows that the dihedral CCNO angle is not exactly equal to 0°.

From our calculations in this work we have concluded that a metal cluster surface with more than 10 atoms does not improve the results. This is in agreement with previous works performed in our laboratory [9–11], and by Lamoen et al. [12].

3.2. Computational details

Works by Scott and Radom [13] and Wong [14] showed that DFT consistently predict harmonic vibrational frequencies in better agreement with observed fundamentals. After optimisation of the molecular geometries at the SVWN/LANL2DZ2 level of theory, DFT harmonic frequencies were computed at the same level. The SVWN exchange-correlation functional, also known as the local spin density approximation (LSDA) consists of Slater's local spin density exchange functional [15] and the correlation functional by Vosko et al. [16]. The LANL2DZ basis set used throughout corresponds to the D95 basis set on first row atoms and the Los Alamos ECP plus DZ on Ag [17]. Scaling of the harmonic frequencies due to the anharmonicity of the molecules is described in the text. All DFT calculations

were performed using the Gaussian 98 program package [18].

4. Results and discussion

4.1. IR and Raman analysis of 6-Nchr and relative compounds

The spectral analysis of 6-Nchr was performed on the basis of both the IR and Raman data and the spectra of various relative compounds, pyrene, fluorene and their corresponding nitro derivatives (see Table 1). This analysis is useful to precise the band assignment of the fundamentals and to distinguish vibrations close and far from the nitro coordination site. A correct assignment is particularly important to interpret the surface-enhanced vibrational spectra, Raman (SERS) and infrared (SEIRA).

In the IR spectrum of 6-nitrochrysene in Fig. 2, the band at 1356 cm^{-1} is assigned to a $\nu_s NO_2$ mode and the band at 1513 cm^{-1} corresponds to $\nu_{as} NO_2$; both bands display a strong relative intensity. The asymmetry and broadness of the first band suggests the existence of another mode probably involving the nitro group: the νCN vibration. This mode has been traditionally ascribed to bands in the 830–870 cm^{-1} region in nitro aromatic compounds. One could expect that this vibration shifts to higher frequency when the NO_2 group is coplanar to the aromatic moiety, which is the case in 6-Nchr. The band corresponding to the in plane bending of the NO_2 group, expected in the 530–580 cm^{-1} spectral region, has not been observed. The IR spectrum of 6-Nchr is well resolved and displays several isolated bands which could be useful for SEIRA and reflection-absorption infrared studies (RAIRS).

The aromatic νCC modes are normally observed between 1700 and 1400 cm^{-1}. The spectral shift to higher energy of several modes by nitro substitution, suggests an energy reinforcement of the CC bonds. This situation is caused by a π electronic redistribution imposed by the electron acceptor characteristic of the nitro group. Spectral shifts to lower energy are attributed to molecular fragments far from the coordination site. Bands observed only in the spectra of 6-nitrochrysene and 1-nitropyrene between 1530 and 1580 cm^{-1} are attributable to inter-ring νCC modes; these bands are not observed in fluorene where there is no this kind of bonds. Bands observed only in the spectra of the nitro derivatives at about 1420 cm^{-1} are ascribed to νCC/νCN coupled modes.

In plane deformation CH modes (δCH) are expected in the 1350–1000 cm^{-1} spectral region (δCH). Sharp and rather weak bands between 1360 and 1300 cm^{-1} are ascribed to these modes. Some bands of chrysene (1145 and 976 cm^{-1}) shift or disappear (1302 and 1082 cm^{-1}) by nitro substitution which indicates that they belong to the molecular moiety close to the substitution site. The fact that some bands are not observed in the spectrum of 6-Nchr could be associated to an anchorage effect induced by an interaction between the oxygen atoms of the nitro group and the adjacent H atoms. Other bands observed in chrysene and 6-Nchr but not in pyrene and fluorene at 1266 and 1254, 976 and 988 cm^{-1}, and 703 cm^{-1} of 6-Nchr are assigned to δCH modes of the bay fragments; these fragments are not in the structure of pyrene and fluorene.

The bands which remain with the same spectral shape are assigned to δCH modes far from the NO_2 group. Out of plane CH modes ρCH are observed between 1000 and 600 cm^{-1}. Ring deformations (δCCC) are expected in the region of the lower frequency. At least three medium bands at 896, 789 and 703 cm^{-1} are only observed in the spectrum of 6-Nchr; this is probably due to a molecular symmetry descent imposed by the NO_2 group. Spectral changes observed in the weak bands at 636 and 612 cm^{-1} are associated with δCCC modes. These modes normally display bands with low relative intensity; the frequency shift is probably due to a π electronic redistribution caused by the NO_2 group.

The observed equivalence of the infrared and Raman bands of the nitro compound is due to the low structural symmetry (D_{2h} in chrysene and C_1 in 6-Nchr). Thus, the Raman spectral assignment follows the same logic used for the IR spectral analysis.

The UV-absorption in Fig. 2 is in resonance with the 325 nm laser line which allowed us to obtain resonance Raman scattering (RRS). The Raman spectrum obtained outside the absorption band with the 514.5 nm laser line is also shown in Fig. 2. The spectral shape of the resonance Raman spectrum, in particular the increased relative intensity of the ring bands in the region 1500–1650 cm^{-1}, allowed us to confirm both most of the aromatic modes assignment and to propose that these normal modes belong to symmetric species. The most probable bands assignment is given in Table 1. In general the calculated intensities and frequencies and description of the different normal modes are in agreement with current experimental assignment.

4.2. Surface-enhanced Raman spectra of the 6-Nchr–Ag system

About 20 nm of 6-Nchr were deposited onto a 6 nm Ag island film. The best SERS spectrum was obtained by using the 633 nm laser line and 10 μW laser power, after washing the sample with a mixture of CH_2Cl_2 and ethanol. This spectrum should correspond to the molecules directly adsorbed on the surface. The Raman spectrum of solid 6-Nchr, and the SERS spectrum of 6-Nchr deposited onto the Ag surface obtained under the present experimental conditions, are shown in Fig. 3. Frequencies are listed in Table 2.

The SERS spectrum, Fig. 3, shows all vibrational modes seen in the Raman spectrum (bottom), with variations in

Table 1
Infrared and Raman frequencies (cm^{-1}) for some polycyclic aromatic hydrocarbons PAHs and nitro-PAHS in the 1700–200 cm^{-1} spectral region

Fluorene		2-Nitrofluorene		Chrysene		6-Nitrochrysene		Pyrene		1-Nitropyrene		Assignment
IR	Raman	IR	Raman	IR	Raman	IR	Raman	IR	Raman	IR	Raman	
1650		1655		1620	1622	1629	1629	1648	1643	1643		νCC
							1607		1627	1627	1623	
1594	1610	1614	1613	1599	1603	1602	1576	1595	1593	1594	1591	νCC
1574	1576	1593	1592									$\nu CC_{pentacycle}$
									1563			
					1575			1552	1550	1555	1556	$\nu CC_{inter\text{-}ring}$
				1518		1533		1524		1544		$\nu CC_{inter\text{-}ring}$
		1520	1513			1513	1527			1511	1501	$\nu_{as}NO_2$
1477	1478	1471	1480	1489		1488		1487		1484	1482	νCC
								1466		1458	1459	$\nu CC_{inter\text{-}ring}$
								1450				$\nu CC_{inter\text{-}ring}$
1447		1450		1437	1433	1440	1435	1432		1432		νCC
		1423	1424			1421	1421			1419	1419	νCC + νCN
1401												νCC + νCN
								1406	1406	1406	1404	$\nu CC_{inter\text{-}ring}$
1388	1399	1397	1396		1382	1373	1387				1386	νCC
1342	1344			1362	1364		1372					δCH
		1335	1336			1356	1356			1332	1327	$\nu_s NO_2$ + νCN
							1328			1313	1310	$\nu_s NO_2$ + νCN
1311	1325				1332			1312				δCH
1299	1293		1283	1302								δCH
				1266	1255	1254	1259					δCH_b
1235	1235	1235	1232	1235	1229			1239	1240	1239	1238	δCH
1219		1206					1219			1222	1219	δCH + νCC
1189	1192	1186	1185	1194		1199		1182		1183	1189	δCH
1156	1152	1157	1156	1145	1163	1156	1155	1136	1143	1155	1152	δCH
1125		1125	1123									CH_2 def.
1108		1107										CH_2 def.
1091		1074	1072	1082				1095		1090	1088	δCH
1028			1028	1033	1043	1047		1064	1067	1041	1041	δCH
				1025	1019		1023					ρCH
1019	1021											CH_2 def.
1000		1005										CH_2 def.
				976		988	987			974		
954		963		959		962		952		957		δCH
		950		943		949				950		
		933										CH_2 def.
913		912	913					911		908		ρCH
876		887			880	896		892		882		
860	844	842	832	863		865		833	840	847		ρCH
		803	804	814		818	823		803	823		ρCH
788		780	782		770	789		779		799	797	ρCH
738	741	741	748	757		753	768	750		756	753	ρCH
										732	731	ρCH
				sh		703	703					ρCH_b
								705		703		ρCH
697												$\delta CCC_{pentacycle}$
		686		678	680	681	680	675		678		ρCH
633		638	637			636				635	632	δCCC
624						612				606		

both the relative intensity and frequencies, Table 2. The NO_2 bands observed in the 1500–1530 and 1300–1340 cm^{-1} spectral region in the SERS spectrum are the most influenced by the surface effect. In particular, the observed frequency shifts indicate that the NO_2 group probably interacts with the surface; this effect is not observed in the case of the chrysene moiety bands. At least one of the bands in the 1300–1340 cm^{-1} should be ascribed to a νCN mode, suggesting that the surface interaction induces a π-electronic redistribution mainly around both the nitro group and the aromatic part in the vicinity of the substitution site. This interaction is very similar to that of nitrobenzene [19], whose $\nu_s NO_2/\nu$CN band is shifted to lower frequencies upon adsorption on an Au film through the oxygen atoms. These results suggest that the interaction with the surface mainly occurs through the NO_2 fragment. We have not observed in

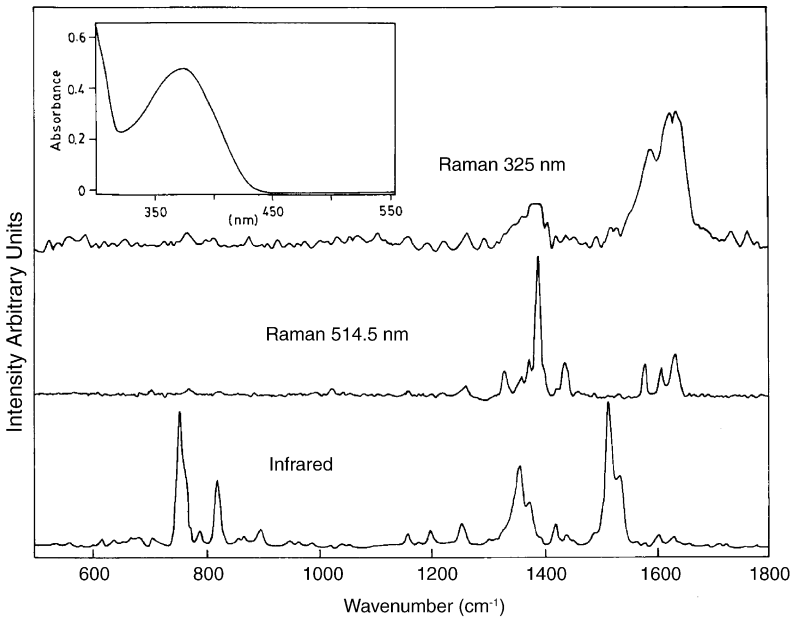

Fig. 2. Raman resonance scattering (RRS) (325 nm), Raman (514.5 nm) and infrared spectra of the solid 6-nitrochrysene. The inset shows the absorption spectrum of 6-Nchr.

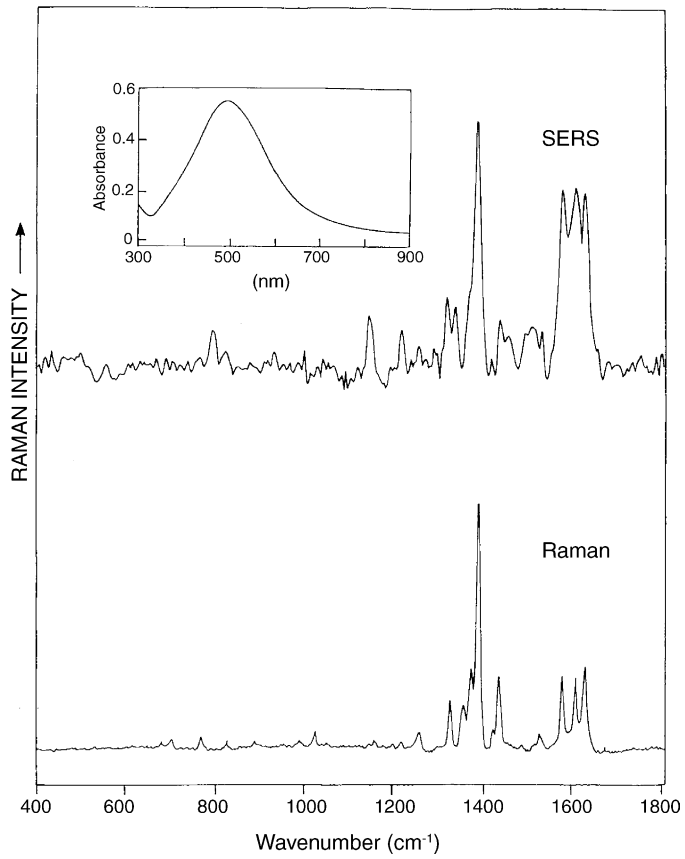

Fig. 3. SERS spectrum of 10 nm 6-nitrochrysene film deposited on 6 nm of Ag islands film at 633 nm irradiated with 10 μW and washed with CH_2Cl_2 and ethanol, and Raman spectrum of the solid 6-nitrochrysene (bottom). The inset shows the plasmon absorption spectrum of 6 nm Ag island films.

Table 2
Raman and surface-enhanced Raman scattering frequencies of 6-nitrochrysene in the 1700–500 cm^{-1} spectral region

Raman	SERS
1629	1627
1607	1607
1576	1577
1527	1530
	1508
	1455
1435	1435
1421	1417
1387	1387
1372	
1356	1338
1328	1320
1259	1259
1219	1216
1155	1142
1023	997
987	
823	819
	791
768	
703	
680	

Table 3
DFT calculated frequencies and intensities for the SERS spectra of the free (A) and frozen (B) 6-Nchr/Ag surface models in the 1700–500 cm^{-1} spectral region

SERS	Model A		Model B	
	Frequency	Intensity	Frequency	Intensity
	1602	74	1602	18
1627	1588	1520	1583	186
	1576	93	1576	102
1607	1564	1578	1564	474
1577	1548	756	1545	224
1530	1497	1214	1506	230
	1492	6	1491	10
1508	1449	213	1453	18
1455	1426	2815	1427	250
1435	1408	671	1413	90
1417	1406	70	1408	6
1387	1398	3291	1396	92
	1379	506	1380	140
	1368	54	1368	106
1338	1351	1903	1352	384
1320	1309	217	1307	76
	1274	911	1295	654
1259	1239	1100	1270	114
1216	1218	617	1222	134
	1207	51	1218	1022
	1202	218	1209	132
	1191	448	1200	3490
	1153	30	1156	220
1142	1142	73	1143	1160
	1123	1	1126	12
	1111	277	1120	846
	1104	0	1105	108
	1065	51	1076	268
	1046	17	1055	8
	1016	4	1021	152
997	1005	59	1007	16
	964	4	980	2
	962	22	969	0
	950	5	967	0
	943	6	952	0
	924	4	928	0
	891	10	917	2
	877	7	878	118
	868	10	873	0
	844	8	846	0
	839	8	843	4
	823	9	833	4
819	822	36	824	16
	797	4	802	60
	789	3	795	4
791	762	38	771	0
	737	48	739	17
	732	5	736	0
	717	29	722	0
	676	114	685	548
	667	49	679	16
	656	18	659	4
	618	378	651	8

the SERS spectrum new bands in the 200–300 cm^{-1} spectral region, where the metal ligand νAg–O mode should appear [8]; this fact suggests that the interaction is rather weak.

According to the SERS selection rules, the spectral profile of the adsorbate is strongly dependent on the orientation of the main molecular axes with respect to the surface. In fact, those modes with a higher perpendicular polarisability component with respect to the surface will be enhanced the most [20–22]. Thus, SERS intensities provide valuable information about the molecular orientation that the adsorbate adopts once adsorbed on the metal surface. Modifications of the relative intensity of several bands by surface effect suggest a preferential orientation of the adsorbate onto the surface. In fact, most of the in plane bands of the chrysene moiety (νCC bands in the 1550–1650 cm^{-1} spectral region and the δCH and νCC modes in the 1100–1400 cm^{-1} spectral region) increase their relative intensity by surface effect. No evident intensity changes of the out of plane ρCH bands below 1050 cm^{-1} are observed in the SERS spectrum. We have intended to obtain the SERS spectrum of the precursor chrysene by using the same experimental conditions used for 6-Nchr without successful. On the other hand the band of the asymmetric νNO_2 mode around 1510 cm^{-1} displays an intensity increasing stronger than that observed for the symmetric band in the region 1320–1350 cm^{-1}. These results suggest that the interaction adsorbate substrate occurring through the NO_2 group concerns mainly one of the oxygen atoms. Thus, we partially conclude that the most probable orientation of 6-Nchr on the Ag surface is rather tilted with the nitro group interacting with the metal through an oxygen atom in a monodentate orientation (Fig. 1). This asymmetric interaction of 6-Nchr with the surface may be induced by the steric hindrance of the ring adjacent to that of the nitro group, see Fig. 1.

4.3. Theoretical calculations

In general, the optimised geometry of the whole system shows that the adsorbate is not exactly perpendicular to the surface constituted by two or more Ag atoms, being the interaction always verified through the oxygen atoms of the nitro group. The optimisation of the geometry concerning the surface produces in all cases a globular stereochemistry, that is, the planarity of the initial surface model disappears. The more Ag atoms in the cluster, more globular is the surface after optimisation, thus, the position of the adsorbate on the surface becomes perpendicular, see Fig. 1. If so, the best theoretical Raman spectra should be that obtained taking into account a geometry optimisation with the larger number of Ag atoms of the surface.

In Table 3, we display the Raman calculated frequencies and intensities of the two models described in Fig. 1. The calculated harmonic frequencies are overestimated due to basis set truncation, neglect of electron correlation and mechanical anharmonicity. Various scaling strategies exist for bringing the computed frequencies into greater coincidence with observed wavenumbers. Here, we have employed the homogeneous scaling, by using the empirical scaling factor 0.961, as suggested by Scott and Radom [13], and Wong [14].

The adsorbate substrate distance resulted to be 2.14 Å for the interacting model in which the whole system was optimised. This distance was fixed to 2.36 Å for the model where both the adsorbate and substrate are frozen; this distance corresponds to the atomic radii sum. Regarding the shape of both calculated spectra as well as the relative intensities observed in Fig. 4 it is possible to see that the best representation corresponds to the fully optimised model. Finally, the calculation predicts an important coupling between several normal modes, which is expected in extended π-electron-delocalised molecular systems.

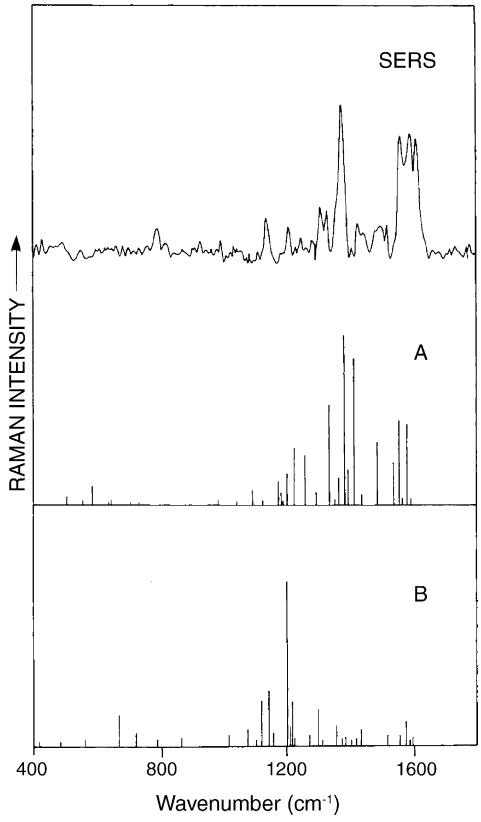

Fig. 4. Experimental SERS spectrum and DFT calculated SERS spectra of the free (A) and frozen (B) 6-nitrochrysene/Ag surface models.

5. Conclusions

The SERS study allowed us to conclude that 6-nitrochrysene interacts with the Ag island film surface through the NO_2 fragment, adopting a preferential perpendicular orientation onto the surface. DFT calculations support both the experimental spectral assignment for SERS and the perpendicularity of the adsorbate position onto the surface as well as the interaction adsorbate substrate through the nitro fragment.

Acknowledgements

Authors acknowledge projects 1010867 and 7010867 from FONDECYT for financial support. RK acknowledges generous allocation of computer time at the Norddeutscher Verbund für Hoch- und Höchstleistungsrechnen (HLRN), Hannover, Berlin and at the Hochschulrechenzentrum, Universität Oldenburg. GDF acknowledges project 010203 from DGI Universidad de Playa Ancha.

References

[1] C.L. Ritter, S.J. Culp, J.P. Freeman, M.M. Marques, F.A. Beland, D. Malejka-Giganti, Chem. Res. Toxicol. 15 (4) (2002) 536.
[2] S.T. Lin, Y.F. Jih, P.P. Fu, J. Org. Chem. 61 (1996) 5271.
[3] J.S. Li, P.P. Fu, J.S. Church, J. Mol. Struct. 550–551 (2000) 217.
[4] S.R. Landhoff, C.W. Bauschlicher Jr., D.M. Hudgins, S.A. Sandford, A.J. Allamandola, J. Phys. Chem. 102 (1998) 1632.
[5] N. Juchnovski, G.N. Andreev, Bulg. Acad. Sci. 16 (1983) 389.
[6] E.A. Carrasco-Flores, R.E. Clavijo, M.M. Campos-Vallette, R.F. Aroca, Spectrochimica Acta A (2004) in press.
[7] E.A.F. Carrasco, R.E. Clavijo, M. Campos-Vallette, R. Aroca, J. Appl. Spectrosc. 58 (2004) 555.
[8] E.A.F. Carrasco, M. Campos-Vallette, N.P. Inostroza, P. Leyton, G.F. Díaz, R.E. Clavijo, J.V. García-Ramos, C. Domingo, S. Sánchez-Cortés, R. Koch, J. Phys. Chem. A 107 (2003) 9611.
[9] M. Saavedra, M. Campos-Vallette, R.E. Clavijo, F. Mendizábal, G. Díaz, J.V. García-Ramos, S. Sánchez-Cortés, Vib. Spectrosc. 32 (2003) 155.
[10] M.M. Campos-Vallette, R.E.C. Clavijo, J. Costamagna, J. Canales, G.F. Díaz, F.E. Mendizábal, J.M. Ramírez, M.S. Saavedra, Vib. Spectrosc. 23 (2000) 39.
[11] M.S. Saavedra, F. Mendizábal, M.M. Campos-Vallette, R.E.C. Clavijo, G.F. Díaz, Vib. Spectrosc. 18 (1998) 25.
[12] D. Lamoen, P. Ballone, M. Parrinello, Phys. Rev. B 54 (1996) 5097.

[13] A.P. Scott, L. Radom, J. Phys. Chem. 100 (1996) 16502.
[14] M.W. Wong, Chem. Phys. Lett. 256 (1996) 391.
[15] J.C. Slater, Quantum Theory of Molecular and Solids, 4, McGraw-Hill, New York, 1974.
[16] S.H. Vosko, L. Wilk, M. Nusair, Can. J. Phys. 58 (1980) 1200.
[17] T.H. Dunning Jr., P.J. Hay, in: H.F. Schaefer, III (Ed.), Modern Theoretical Chemistry, 3, Plenum Press, New York, 1977pp. 1–27; (b) P.J. Hay, W.R. Wadt, J. Chem. Phys. 82 (1985) 299.
[18] M.J. Frisch, G.W. Trucks, H.B. Schlegel, G.E. Scuseria, M.A. Robb, J.R. Cheeseman, V.G. Zakrzewski, J.A. Montgomery, R.E. Stratmann, J.C. Burant, S. Dapprich, J.M. Millam, A.D. Daniels, K.N. Kudin, M.C. Strain, O. Farkas, J. Tomasi, V. Barone, M. Cossi, R. Cammi, B. Mennucci, C. Pomelli, C. Adamo, S. Clifford, J. Ochterski, G.A. Petersson, P.Y. Ayala, Q. Cui, K. Morokuma, D.K. Malick, A.D. Rabuck, K. Raghavachari, J.B. Foresman, J. Cioslowski, J.V. Ortiz, B.B. Stefanov, G. Liu, A. Liashenko, P. Piskorz, I. Komaromi, R. Gomperts, R.L. Martin, D.J. Fox, T. Keith, M.A. Al-Laham, C.Y. Peng, A. Nanayakkara, C. Gonzalez, M. Challacombe, P.M.W. Gill, B.G. Johnson, W. Chen, M.W. Wong, J.L. Andres, M. Head-Gordon, E.S. Replogle, J.A. Pople, Gaussian, Inc., Pittsburgh, PA, USA, 1998.
[19] W. Karcher, R.J. Fordham, J.J. Dubois, Glaude, in: P.G.J.M., Ligthart, J.A.M., Spectral Atlas of Polycyclic Aromatic Compounds, vol. 13, D. Reidel Publ. Co., Dordrecht, Boston, Lancaster, 1985, 227 pp.
[20] M. Moskovits, Rev. Mod. Phys. 57 (1985) 783.
[21] S. Corni, J. Tomasi, J. Chem. Phys. 116 (2002) 1156.
[22] R.F. Aroca, R.E. Clavijo, M.D. Halls, H.B. Schlegel, J. Phys. Chem. A 104 (2000) 9500.